Journal of Environmental Management 255 (2020) 109850

Contents lists available at ScienceDirect

Journal of Environmental Management

journal homepage: http://www.elsevier.com/locate/jenvman

Research article

Effect of calcium addition on the formation and maintenance of aerobic granular sludge (AGS) in simultaneous fill/draw mode sequencing batch reactors (SBRs)

Antônio Ricardo Mendes Barros, Silvio Luiz de Sousa Rollemberg, Clara de Amorim de Carvalho, Ian Holanda Herbster Moura, Paulo Igor Milen Firmino, André Bezerra dos Santos *

Department of Hydraulic and Environmental Engineering, Federal University of Ceará, Fortaleza, Ceará, Brazil

ARTICLE INFO

Keywords:
Aerobic granular sludge
Simultaneous fill/draw mode SBR
Calcium addition

ABSTRACT

This work investigated the effect of Ca^{2+} (100 mg L^{-1}) addition on the formation and maintenance of aerobic granular sludge in a simultaneous fill/draw mode sequencing batch reactor (SBR), operated with a low liquid upflow velocity (0.92 m h^{-1}), in order to verify if Ca^{2+} presence compensates the low selection pressure imposed. Additionally, carbon and nutrients removals, granules characteristics and microbial community were evaluated. For this, two SBRs (R1, control, and R2, Ca^{2+}-supplemented) were operated (6-h cycle). In general, Ca^{2+} supplementation affected positively the sludge settleability, although a larger fraction of inert solids was found in the granules. The total extracellular polymeric substances were the same for both reactors, and no remarkable differences were observed between their polysaccharides and proteins contents. Overall, Ca^{2+} addition in a simultaneous fill/draw mode SBR neither accelerated the granule formation nor improved the operational performance. The microbial community structure, especially in terms of bioactivity, was not affected as well. Therefore, the effect of divalent cations might be more pronounced in conventional SBRs, in which the selection pressure is higher.

1. Introduction

Aerobic granular sludge (AGS) is considered a promising technology for biological wastewater treatment, not only because of its excellent resistance and settleability, but also because it enables the simultaneous removal of pollutants (carbon, nitrogen and phosphorus) (Lochmatter et al., 2013). Additionally, when compared to conventional activated sludge (CAS) systems, AGS technology presents lower operational costs (20–25%) and electricity expenses (23–40%) as well as smaller space requirements (50–75%) (Adav et al., 2008; Bengtsson et al., 2019; Nereda, 2017).

Most of the investigations on AGS cultivation and maintenance were conducted in conventional sequencing batch reactors (SBRs), in which the steps of filling, reaction, settling and decanting are a function of time (Jiang et al., 2003; Liu et al., 2010a). Simultaneous fill/draw mode (simultaneous filling and decanting - reaction - settling) is another way to operate SBRs, i.e. at constant volume. In this system, the feeding solution is pumped into the bottom of the reactor and, as the influent liquid rises, the decanting takes place at the top (Derlon et al., 2016; Wang et al., 2018b). Although most of the AGS full-scale wastewater treatment plants (WWTP) are currently designed to be operated at constant volume, in which case the most notorious example is the Nereda® technology, there is a shortage of studies regarding this type of operational regime (Derlon et al., 2016; Wang et al., 2018b; Nereda, 2017).

In this context, it has been reported that, in constant-volume SBRs, granulation is achieved through high liquid upflow velocity (16 m h^{-1}), which causes the washout of floccular sludge (Derlon et al., 2016). However, Wang et al. (2018b) obtained more than 50% of granular sludge (diameter larger than 0.2 mm) operating lab-scale constant-volume SBRs with a liquid upflow velocity as low as 0.67 m h^{-1}. This seems to indicate that granulation could be possible with lower liquid upflow velocities, which would require less powerful pumps, decreasing the operational costs.

It is possible that the addition of divalent cations could compensate for the low selection pressure generated by low feeding velocities,

* Corresponding author. Department of Hydraulic and Environmental Engineering. Campus do Pici, Bloco 713. Pici., CEP: 60455-900, Fortaleza, Ceará, Brazil.
E-mail address: andre23@ufc.br (A.B. dos Santos).

https://doi.org/10.1016/j.jenvman.2019.109850
Received 5 July 2019; Received in revised form 26 September 2019; Accepted 10 November 2019
Available online 21 November 2019

allowing granulation to occur. Several researchers have reported the benefits of such ions for granulation. Jiang et al. (2003), working with a conventional SBR, found that calcium addition led to a faster granule formation (reduction from 32 to 16 days) with larger granules (increase from 2 to 2.8 mm), a greater biomass retention (increase from 2.0 to 7.9 g SS·L^{-1}), and a better settleability (sludge volume index at 30 min, SVI_{30}, improved from 150 to 100 mL g^{-1}). Liu et al. (2010a) used magnesium in a conventional SBR and also observed a decrease in the granulation time (from 32 to 18 days), an increase in the granule size (from 1.8 to 2.9 mm), and a greater biomass retention (from 6.8 to 7.6 g SS·L^{-1}), although settleability remained almost constant (SVI_{30} between 20 and 25 mL g^{-1}).

Overall, it is suggested that the divalent cations act in three ways on AGS systems: (I) they work as a bridge between negatively charged polysaccharides and bacterial surfaces, facilitating aggregation; (II) they increase the extracellular polymeric substances (EPS) production; and (III) they precipitate and serve as a surface to which bacteria can attach (Jiang et al., 2003; Ren et al., 2008). In addition, some of these ions are important cofactors of enzymes involved in carbon, nitrogen, and phosphorus removal metabolism (Liu and Tay, 2002).

Moreover, there is little information concerning the effect of calcium on the microbial community of AGS. Calcium has been reported to have a negative effect on granule bioactivity, decreasing its oxygen utilization rate (Liu et al., 2010a). It was also reported that calcium precipitation in the granules core prevents the survival of microorganisms in this region due to mass transfer limitations (Ren et al., 2008).

Therefore, the present study investigated the effect of Ca^{2+} addition on the formation and maintenance of AGS in a simultaneous fill/draw mode SBR, operated with a low liquid upflow velocity (0.92 m h^{-1}), in order to verify if Ca^{2+} presence compensates for the low selection pressure imposed. Furthermore, the carbon, nitrogen, and phosphorous removals, operational stability, granules characteristics, and microbial community were also evaluated.

2. Material and methods

2.1. Experimental set-up

Two identical simultaneous fill/draw mode SBRs were used. The reactor R1 was used as control (no Ca^{2+} addition), while the reactor R2 was supplemented with calcium (100 mg L^{-1} of Ca^{2+} from $CaCl_2$). The reactors had a diameter of 100 mm and a total height of 1 m, i.e. a height to diameter ratio (H/D) of 10. Their working volume, hydraulic retention time (HRT) and volumetric exchange ratio were 7.2 L, 12 h and 50%, respectively. The feeding solution was pumped by peristaltic pumps (Masterflex model BTG 2344), at a liquid upflow velocity of 0.92 m h^{-1}, into the bottom of the reactors, while the treated wastewater was decanted simultaneously from the top.

The total cycle of both SBRs was the same (6 h), which, at Stage I, consisted of simultaneous filling/decanting (30 min), anaerobic reaction (90 min), aerobic reaction (210 min), and settling (30 min). At the following stages, the settling time was gradually decreased from 30 to 15 (Stage II), 10 (Stage III), and, finally, 5 min (Stage IV). Each stage was maintained for approximately 6 weeks. In order to keep the total cycle constant, the time decreased in the settling step was added to the aerobic reaction step. The aeration rate used was 10.0 L min^{-1}, resulting in a superficial gas velocity of 2.12 cm s^{-1} and a dissolved oxygen (DO) concentration above 50% of the saturation value (6–8 mg L^{-1}). No stirring was used during the anaerobic phase.

The synthetic wastewater used was composed of 800 mg COD·L^{-1} of ethanol as carbon source, 100 mg L^{-1} of N–NH_4^+ (from NH_4Cl) as nitrogen source, 10 mg L^{-1} of P-PO_4^{3-} (from KH_2PO_4) as phosphorus source, 1 g $NaHCO_3$·L^{-1} as alkalinity source, and 1 mL L^{-1} of a trace element solution, prepared according to Rollemberg et al. (2019). As aforementioned, the feeding solution of R2 was supplemented with 100 mg L^{-1} of Ca^{2+} (from $CaCl_2$). The synthetic wastewater used was stored in a refrigerator at 4 °C in order to prevent its degradation.

The seed sludge was collected from a CAS system of a WWTP located in Fortaleza, Ceará, Brazil. The initial concentration of the mixed liquor suspended solids (MLSS) of R1 and R2 was about 2 g L^{-1}, achieved by the introduction of approximately 3.6 L of sludge. The initial sludge volume index at 30 min (SVI_{30}) was 110 mL g^{-1}. The operational temperature of the experiment was 28 ± 2 °C.

2.2. Analytical methods

In order to evaluate the system performance in terms of organic matter and nutrients, the following parameters were determined: COD, nitrogen in the forms of ammonium (N–NH_4^+), nitrite (N–NO_2^-), and nitrate (N–NO_3^-), and phosphorous in the form of phosphate (P-PO_4^{3-}). The pH, DO, temperature, alkalinity, total hardness, and calcium concentration were used as operational parameters. All analyses were conducted according to the *Standard Methods for the Examination of Water and Wastewater* (APHA, 2012) twice a week. The amount of nitrogen assimilated by the biomass per day was also estimated (Wan et al., 2009). Since no regular sludge discharge from the reactors was done, this fraction was disregarded in the mass balance calculation.

The granulation process was evaluated in terms of sludge settleability by using the dynamic sludge volume index (SVI), a modified version of the SVI at the times of 5 (SVI_5), 10 (SVI_{10}), and 30 (SVI_{30}) min (Schwarzenbeck et al., 2005). This analysis was also carried out twice a week.

2.3. Physical, chemical and morphological characterization of the biomass

The physical resistance (shear test) analysis of the granules followed the methodology described by Nor-Anuar et al. (2012). The granules (>0.2 mm) were subjected to a shear force caused by an approximate rotation of 200 rpm for 10 min. The defragmented fraction identified was expressed in terms of the stability coefficient (S). This coefficient was classified into three categories: very resistant ($S < 5\%$), resistant ($5\% \leq S \leq 20\%$), and non-resistant ($S > 20\%$). Therefore, the lower the values of S (%), the higher the stability of the aerobic granules.

The granule shape and formation over the experiment was monitored using an optical microscope as well as a scanning electron microscope combined with an energy dispersive X-ray detector (SEM-EDX) (Inspect S50 - FEI). The sample preparation followed the methodology described elsewhere (Motteran et al., 2013).

The EPS content was also quantified. For this, initially, 5 mL volume of mixed liquor suspended solids (MLSS) of the reactors was collected, and the EPS were extracted by applying alkaline conditions (pH > 10, with the addition of 5 mL of 1 mol L^{-1} NaOH), followed by high temperature (30 min at 80 °C) and sonication (5 min at 55 kHz) (Tay et al., 2001). A modified Lowry method was used to calculate proteins content (PN), and the phenol-sulfuric acid method was used to calculate polysaccharides content (PS) (Long et al., 2014). EPS were determined as the sum of PN and PS.

2.4. DNA extraction, 16S rRNA gene amplicon sequencing and data processing

Samples from the mixed liquor (at the end of the aeration reaction) were collected on the 205th day of operation (maturation phase, end of Stage IV), and DNA was extracted using PowerSoil® DNA isolation kit (MoBio Laboratories Inc., USA) according to manufacturer's instructions. All analytical procedure is described elsewhere (Rollemberg et al., 2019).

2.5. Statistical methods

Statistical analyses were performed with Statgraphics Centurion XV

computer software applying the Mann-Whitney Rank Sum test to compare the performance of the reactors at a confidence level of 95%.

3. Results and discussion

3.1. Granulation through settleability characteristics

The values of SVI_5, SVI_{10}, and SVI_{30} over time for the two simultaneous fill/draw mode SBRs are shown in Fig. 1. It is worth noting that the first sludge sample for SVI determination was collected approximately two days after the inoculation. The difference between the seed sludge SVI_{30} and the first SVI_{30} registered in Fig. 1 was due to a sludge washout which occurred in this time interval.

Overall, it can be observed that the values of SVI_5, SVI_{10}, and SVI_{30} became smaller with the settling time decrease. This demonstrates that biomass settleability improved over time, which is a typical behavior of the evolution of flocculent sludge to granular sludge. The SVI values observed in Stage IV are similar to those found in reports on both conventional and constant volume SBRs, which presented SVI_{30} values between 30 and 80 mL g^{-1} (Derlon et al., 2016; Liu et al., 2010b; Long et al., 2014).

Furthermore, on the 100th day, the sludge of R2 reached SVI_{30} values lower than 50 mL g^{-1}, while the sludge of R1 remained with SVI_{30} above 100 mL g^{-1}. Even after stabilization (Stages III and IV), the control reactor R1 remained with SVI_{30} higher than the calcium-supplemented reactor R2 (R1: $SVI_{30} > 50$ mL g^{-1}; R2: $SVI_{30} < 50$ mL g^{-1}).

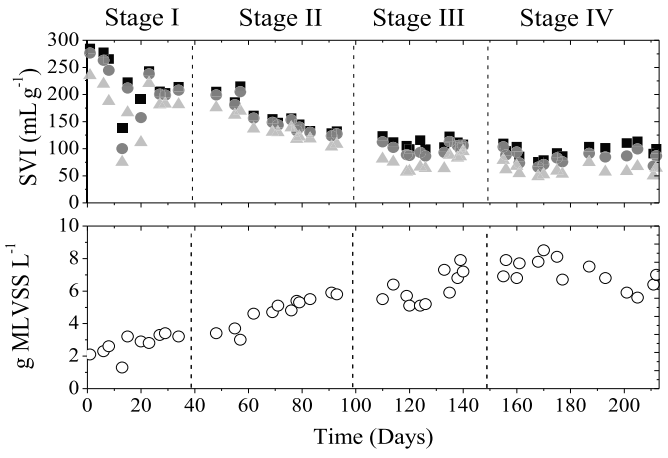

(a)

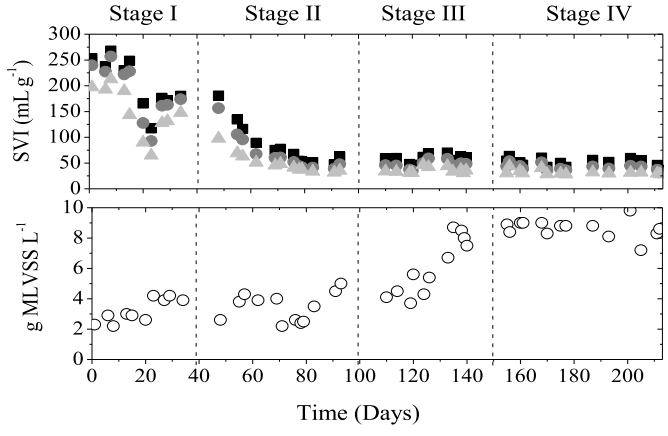

(b)

Fig. 1. MLVSS and SVI values throughout the four operational stages of (a) R1 (control) and (b) R2 (supplemented with Ca^{2+}). (■) SVI_5, (●) SVI_{10}, (▲) SVI_{30} and (○) MLVSS.

It was also observed that the SVI_5 values had greater proximity to the values of SVI_{30} for the reactor R2 compared to R1, indicating that the sludge cultivated in the reactor supplemented with calcium had a greater settleability.

Other studies corroborate the positive influence of calcium on sludge settleability. Liu et al. (2010a) used a continuous dosage of 40 mg L^{-1} de Ca^{2+} in a conventional SBR treating synthetic wastewater and obtained SVI_{30} values around 20 mL g^{-1}. The authors used a seed sludge from a municipal sewage treatment plant and cultivated it for 12 days, using a 75% volumetric exchange ratio and a settling time of 10 min, followed by decanting. In another investigation, Jiang et al. (2003) used a continuous dosage of 100 mg L^{-1} de Ca^{2+} in a conventional SBR treating synthetic wastewater with a settling time of 2 min and found a SVI_{30} average value of 73 mL g^{-1} as well as a reduction in the granulation period from 32 to 16 days. However, the strategies used by these investigations imposed a high selection pressure on the systems, which does not usually happen in real-scale systems.

The mixed liquor volatile suspended solids (MLVSS) concentrations over time are shown in Fig. 1. There was an increase in the MLVSS concentration even at the first stages and with the decrease of the settling time, reaching values of about 8 g MLVSS·L^{-1} for both reactors, indicating a low selection pressure. The observed values are compatible with those reported in the literature for AGS cultivated in conventional SBRs (Li et al., 2009; Zhang et al., 2017). At Stages III and IV, the average sludge retention time (SRT) was 35 and 32 days for R1 and R2, respectively.

Fig. 1 also shows that no significant MLVSS decrease occurred in R1 at Stages I and II, although both reactors reached the same MLVSS concentration at Stage IV. This behavior is unusual for conventional SBR, for which decreases in the settling time are commonly followed by a sludge washout, reaching values between 0.5 and 1 g VSS·L^{-1} (Kończak et al., 2014; Pijuan et al., 2011). It is possible that such a behavior is related to the SBR operation at constant volume, which could have decreased the influence of settling time on the elimination of poor-settling sludge. In these reactors, the liquid upflow velocity might play a more important role in the process.

The MLVSS/MLSS ratios achieved at Stage IV were 0.8 and 0.7 for R1 and R2, respectively. The slightly lower value found in R2 could suggest the occurrence of accumulation of inert material in the sludge, possibly inorganic calcium compounds. Similar behavior in calcium-supplemented granules was reported by Ren et al. (2008), who assessed the cultivation of granules with addition of 40 mg Ca^{2+}·L^{-1} to a conventional SBR during a three-month period. They found MLVSS/MLSS ratios of 0.7 for granules with dimensions between 4 and 6 mm and of 0.85 for those of dimensions between 2 and 2.5 mm, having attributed these results to the accumulation of calcium in the central region of the granules, mainly in the form of $CaCO_3$ precipitates. Liu et al. (2010a) also reported greater accumulation of inert material in the granules supplemented with 40 mg Ca^{2+}·L^{-1} in comparison to those enriched with 40 mg Mg^{2+}·L^{-1} (MLVSS/MLSS ratios of 0.84 and 0.95, respectively, after 110 operational cycles). The investigation was also carried out in conventional SBRs.

At the end of the granulation (Stage IV), for both reactors, more than 96% of the sludge was formed by granules (>0.2 mm) (de Kreuk et al., 2007). This proportion is even larger than the 50% of granular sludge obtained by Wang et al., 2018 operating lab-scale constant-volume SBRs with a liquid upflow velocity as low as 0.67 m h^{-1}. Combined, both studies confirm that it is possible to achieve granulation in constant-volume SBRs with a low liquid upflow velocity. However, contrary to what was hipotesized, calcium addition was not the decisive factor for granulation in the present study, since the control reactor showed a very similar behavior in terms of granule size distribution (Fig. 2). Nevertheless, calcium supplementation increased the

proportion of granules larger than 1 mm (R1: 80%, R2: 90%).

Moreover, the granulometric distribution found in the present study contrasts with the results obtained by Derlon et al. (2016), who worked with a constant-volume SBR (volumetric exchange ratio of 50%) fed with a real and low-strength municipal wastewater. In the end of last operation phase (liquid upflow velocity of 1 m h^{-1} and settling time reduction from 10 to 3 min), they found that 60% of the granules had sizes between 0.25 and 0.63 mm, while only about 15% were larger than 0.63 mm.

The observed difference might be due to the type of substrate, since the present study used ethanol and not real wastewater. The findings of Wang et al. (2018b) corroborate this hypothesis. The authors used simultaneous fill/draw mode SBRs, with a 90% volumetric exchange ratio, and compared a reactor fed with a low-strength sewage (R1) with another one fed with synthetic wastewater containing acetate (R2). In the reactor fed with sewage, the granules reached larger sizes (R1: 0.2–0.8 mm; R2: 0.2–0.6 mm). Thus, it is reinforced that the wastewater composition is a determining factor for the formation of larger and denser particles.

In general, the presence of Ca^{2+} positively affected settleability, although the formed granules had a larger fraction of inert solids. Possibly, the decrease of the settling time and the use of ethanol as carbon source were the factors of greater influence on the granule size.

3.2. General performance of the AGS system during the granulation process

The general performance of R1 and R2 in terms of efficiency and operational stability is shown in Table 1. The removal of organic matter was stable during the phases of biomass selection, biomass aggregation, and settleability reduction (Stages I and II). This pattern was maintained during the stabilization phase (transition between Stages III and IV). During the whole experiment, the efficiencies were higher than 90% for both reactors, with reduced values of standard deviation and no significant difference ($p = 0.20$), revealing a great system stability.

The nitrification process was observed in both systems during the four stages, with values higher than 80%. At Stage II, the nitrification efficiency of the control system R1 reduced significantly (Stage I: $96.7 \pm 9.6\%$, Stage II: $81.9 \pm 10.4\%$). The reactor supplemented with calcium R2 remained stable, showing a reduction in the nitrification capacity only at the last stage (Stage III: $92.4 \pm 7.5\%$, Stage IV: $84.7 \pm 6.6\%$). However, when comparing the reactors during the entire granulation process, no significant statistical difference was found for the nitrification performance ($p = 0.06$).

The observed results concerning nitrification are likely associated with biomass retention. With the increase in MLVSS concentration, the demand for DO would have increased, especially due to the growth of heterotrophic bacteria, considering the biomass endogenous respiration. Since the aeration flow rate was maintained unchanged throughout the experiment, it is possible that there was a shortage of DO in some regions of the formed granules. The lack of oxygen would have affected the activity of nitrifying bacteria (ammonia oxidizing bacteria, AOB, and nitrite oxidizing bacteria, NOB), thus reducing the efficiency of nitrification.

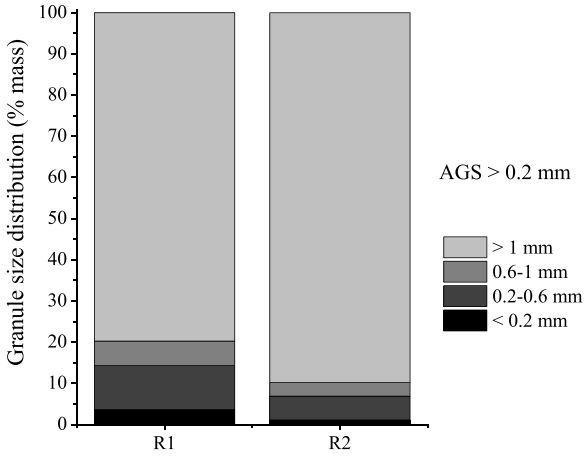

Fig. 2. Granule size distribution (% mass) at the end of Stage IV (190th day) for AGS cultivated in the simultaneous fill/draw mode SBRs R1 (control) and R2 (supplemented with Ca^{2+}).

In fact, there is a correspondence between the biomass increase (Fig. 1) and the drop in nitrification efficiency (Table 1). In R1, there is a decrease in the average nitrification levels from Stage I to II. Concurrently, the most rapid growth of biomass retention in this reactor occurred in Stage II, when the MLVSS concentration increased from 3 to almost 6 g MLVSS·L^{-1}. At the following stages, the growth of biomass retention is more discrete, and the nitrification efficiencies remain stable. As for R2, a decrease in the mean nitrification levels between Stages II and IV was observed. At the same time, rapid growth of biomass retention was observed at Stage III, when the MLVSS increased from 4 to 8 g VSS·L^{-1}.

The different nitrogen fractions of the influent and effluent are also shown in Table 1. Oxidized nitrogen (NOx) fractions were found in the effluent. The amount of NO_3^- in the effluent showed to be considerably higher than that of NO_2^- for both reactors at all stages, indicating that complete nitrification took place. For the mature granules (Stages III and IV), the denitrification efficiency was around 40%. There was no significant difference between the two systems for this process ($p > 0.05$).

The percentages of the main nitrogen removal processes, taking into account the nitrogen fraction assimilated in the sludge, are shown in Fig. 3. At Stage III, where the biomass retention growth was more pronounced, the percentage of nitrogen in the sludge was 19% in R1 and 18% in R2. At Stage IV, R2 maintained values close to those of the previous stage (19%), while a decrease was observed in R1 (14%) due to a small biomass concentration decrease on the 180th day of operation.

Regarding the biological removal of phosphorus, the reactors showed removals lower than 50%, except R1 at Stage II, which were not considered satisfactory when compared with other studies. For example, Wang et al. (2018a) operated a conventional SBR with an anaerobic reaction step followed by an aerobic reaction step with high aeration rates (DO between 7 and 8 mg L^{-1}) and found total phosphorus removal around 98% during the 80 days of operation. They utilized a synthetic wastewater with acetate (220 mg COD·L^{-1}) as the carbon source and ammonia (11–55 mg L^{-1}) as the nitrogen source. The reactor was also supplemented with magnesium (10 mg L^{-1}) and calcium (10 mg L^{-1}), and the total cycle time was of 6 h (filling: 2 min; anaerobic reaction: 120 min; aerobic reaction: 90 min; anoxic reaction: 144 min; settling: 2 min; decanting: 2 min).

The low P removal obtained in the present work is an unexpected outcome, since the use of anaerobic-aerobic cycles usually favors the growth of phosphorus-accumulating organisms (PAOs), with the release of phosphate in the anaerobic phase and its subsequent uptake in the aerobic phase (de Kreuk, 2006). One possible explanation for such result might be the presence of $N–NO_2^-$ and $N–NO_3^-$ in the anaerobic phase. It has been reported that these ions (nitrite and nitrate) cause competition between PAOs and denitrifying heterotrophic microorganisms (DNB), where the latter usually takes advantage for kinetic reasons, therefore interfering negatively in the P removal efficiencies (Chuang et al., 1996). The chosen carbon source might be another factor contributing to the low P removal. Ethanol has been reported as one of the best substrates for heterotrophic denitrification (Pronk et al., 2015). In addition, some works using ethanol reported a higher prevalence of glycogen-accumulating organisms (GAOs) over PAOs (Rollemberg et al., 2019). These observations indicate that ethanol might not favor PAOs as these bacteria (PAOs) compete directly with GAOs and denitrifying heterotrophic microorganisms (Bassin et al., 2012).

Table 1
Operational performance of AGS cultivated in the simultaneous fill/draw mode SBRs R1 (control) and R2 (supplemented with Ca^{2+}).

Reactor		R1				R2			
Stage		I	II	III	IV	I	II	III	IV
Duration (days)		39	60	49	63	39	60	49	63
Settling time (min)		30	15	10	5	30	15	10	5
COD	Influent ($mg{\cdot}L^{-1}$)	985 (123)	776 (107)	694 (86)	694 (149)	985 (123)	776 (107)	694 (86)	694 (149)
	Effluent ($mg{\cdot}L^{-1}$)	31 (24)	54 (38)	21 (17)	28 (15)	35 (22)	37 (20)	31 (23)	44 (24)
	Removal efficiency (%)	94 (2)	93 (5)	97 (2)	96 (3)	96 (2)	95 (4)	96 (3)	93 (4)
Nitrogen fractions	Influent NH_4^+ ($mg\ N{\cdot}L^{-1}$)	114.2 (15.5)	96.5 (8.0)	90.7 (6.2)	92.3 (7.6)	114.2 (15.5)	96.5 (8.0)	92.6 (6.2)	92.3 (7.6)
	Effluent NH_4^+ ($mg\ N{\cdot}L^{-1}$)	3.7 (2.5)	14.9 (6.6)	10.3 (6.4)	10.2 (6.3)	6.9 (5.4)	1.2 (1.4)	7.1 (2.8)	14.5 (8.9)
	Effluent NO_2^- ($mg\ N{\cdot}L^{-1}$)	8.7 (1.4)	8.4 (3.8)	13.1 (5.4)	4.2 (3.6)	6.4 (4.8)	5.3 (2.6)	10.2 (8.3)	2.4 (1.2)
	Effluent NO_3^- ($mg\ N{\cdot}L^{-1}$)	45.1 (15.4)	26.4 (12.2)	25.4 (7.4)	23.7 (6.8)	50.3 (9)	46.7 (10.4)	24.4 (9.1)	21.4 (8.4)
	N in sludge ($mg\ N{\cdot}L^{-1}$)	15.2	11.9	18.3	12.6	16.2	12.2	16.3	18.8
	Nitrification efficiency (%)	96.7 (9.6)	81.9 (10.4)	80.4 (7.6)	83.2 (6.4)	93.9 (19.0)	97.7 (11.8)	92.4 (7.5)	84.7 (6.6)
	Denitrification efficiency (%)	34.8 (8.9)	40.9 (12.3)	26.9 (10.4)	48.5 (10.1)	27.9 (21.2)	35.9 (8.3)	36.4 (9.2)	41.2 (11.0)
pH	Influent	7.4 (0.5)	7.5 (0.3)	7.0 (0.5)	7.5 (0.2)	7.4 (0.5)	7.5 (0.3)	7.0 (0.5)	7.5 (0.2)
	Effluent	7.8 (0.4)	8.0 (0.2)	7.6 (0.3)	7.5 (1.0)	7.5 (0.4)	7.7 (0.2)	7.8 (0.2)	8.0 (0.2)
Total alkalinity	Influent ($mg\ CaCO_3{\cdot}L^{-1}$)	694 (204)	783 (130)	631 (130)	723 (68)	694 (204)	783 (130)	631 (130)	723 (68)
	Effluent ($mg\ CaCO_3{\cdot}L^{-1}$)	275 (172)	457 (157)	312 (116)	367 (165)	177 (137)	283 (91)	353 (61)	354 (84)
Phosphorous	Influent ($mg\ P\text{-}PO_4^{3-}{\cdot}L^{-1}$)	7.5 (0.7)	7.6 (1.0)	6.8 (1.2)	11.1 (1.7)	7.5 (0.7)	7.6 (1.0)	6.8 (1.2)	11.1 (1.7)
	Effluent ($mg\ P\text{-}PO_4^{3-}{\cdot}L^{-1}$)	4.6 (0.7)	3.3 (0.9)	4.2 (1.2)	8.6 (1.5)	4.60 (0.6)	4.0 (0.8)	4.3 (1.0)	5.7 (1.2)
	Removal efficiency (%)	39.1 (10.2)	56.5 (14.0)	37.9 (14.0)	22.6 (8.5)	32.9 (8.2)	47.5 (11.0)	36.1 (10.0)	48.4 (10.0)

The standard deviation is shown in parenthesis.

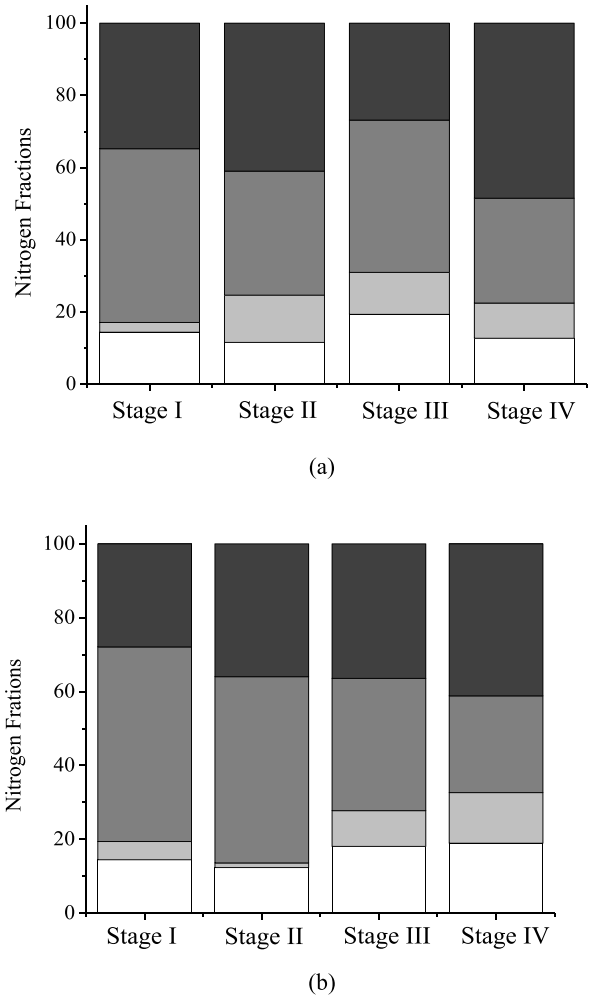

Fig. 3. Distribution of nitrogen fractions under the different operational conditions investigated of (a) R1 (control) and (b) R2 (supplemented with Ca^{2+}). (■) Denitrified, (■) nitrified in the effluent, (■) NH_4^+ in the effluent and (□) nitrogen present in the sludge.

3.3. Characteristics of the granules

The images obtained by optical microscopy and scanning electron microscopy (SEM) at the end of Stage IV are shown in Fig. S1 (Supplementary Material). The granules produced in the control reactor (R1) presented irregular characteristics, with spongy structure, whereas the biomass obtained in the reactor supplemented with calcium (R2) had a uniform circular shape and compact appearance. SEM analysis showed that granules had a very cohesive structure, without many voids, and were well-delineated. These observations were evidenced by the absence of inorganic crystals or organic material differentiated from the amorphous material that enveloped the entire surface of the granules.

In terms of resistance, the stability coefficient (S) values were $27 \pm 5\%$ and $28 \pm 2\%$ for R1 and R2, respectively. Physical resistance is a key parameter to describe the characteristics of microbial granules, since it represents the integrity capacity against the shear stresses imposed. Thus, the biomass formed did not present different characteristics in this aspect based on the classification suggested by Nor--Anuar et al. (2012), according to whom the granules were classified as non-resistant.

Another essential parameter for granule characterization is the EPS structure. The concentrations of PS (polysaccharides) and PN (proteins) at the end of Stage IV are shown in Table 2. PS content was higher than PN content in both reactors. However, the PS/PN ratio of R2 (1.7) was lower than the value found for R1 (2.1).

Jiang et al. (2003) used a conventional SBR supplemented with calcium ($100\ mg\ L^{-1}$), with a volumetric exchange ratio of 50%, and obtained PS/PN ratios of about 0.7 and 1.5 for the control reactor (R1) and the calcium-supplemented reactor (R2), respectively. Such an increase was due to a higher PS production, which was twofold higher when calcium was present (R1: $41\ mg\ g\ VSS^{-1}$, R2: $92\ mg\ g\ VSS^{-1}$), while the PN content was around $60\ mg\ g\ VSS^{-1}$ in both reactors.

The absolute values of PS, PN, and PS/PN ratio presented by Jiang

Table 2
EPS composition (at Stage IV) of AGS cultivated in the simultaneous fill/draw mode SBRs R1 (control) and R2 (supplemented with Ca^{2+}).

Parameter	R1	R2
PS ($mg\ PS\ g^{-1}\ VSS$)	93 ± 8	87 ± 8
PN ($mg\ PN\ g^{-1}\ VSS$)	44 ± 5	50 ± 5
PS/PN	2.1	1.7

et al. (2003) for the calcium-supplemented reactor are similar to those obtained in the present study for reactor R2. However, while Jiang et al. (2003) observed an increase in the total EPS, in the present study, the total EPS were the same for R1 and R2. In addition, no remarkable differences were observed in the amounts of PS and PN. Therefore, the operating conditions of the systems seemed to interfere more than the supplementation of calcium in the EPS profiles observed.

The energy dispersive X-ray (EDX) analysis performed together with the SEM analysis showed that the EPS matrix of the granules were mostly composed of C (R1: 33.5%, R2: 40%) and O (R1: 39.8%, R2: 25%), as well as small concentrations of K, P, Na, Cl, and S. Regarding the calcium content in the EPS, in R1, it was below the detection limit (<0.1%), whereas, in R2, it was 1.1%. Nevertheless, this value was much lower than that reported by Ren et al. (2008) (~14%) in a conventional SBR supplemented with 40 mg $Ca^{2+}{\cdot}L^{-1}$, a smaller concentration than that used in the present study (100 mg $Ca^{2+}{\cdot}L^{-1}$). According to those authors, this accumulation occurred mostly in the form of $CaCO_3$ and led to a severe mass transfer limitation in the aerobic granules. Consequently, the microorganisms were nearly absent in the granule core.

On the other hand, in the present study, calcium precipitation it was not verified by the EDX analysis. In fact, this could be justified by the alkalinity source used ($NaHCO_3$) and the pH of the system (7–8) (Table 1). In this pH range, phosphate is present in $H_2PO_4^-$ and HPO_4^{2-} forms, which have high and intermediate solubility, and bicarbonate, which is highly soluble, is not converted into carbonate at pH below 8.3 (Girard, 2013). Therefore, the probability of calcium precipitation as phosphate or carbonate salts is very low.

In parallel, phosphorus precipitation promoted by calcium addition was not observed as reported by Mañas et al. (2011), who worked with a sequencing airlift batch reactor (SBAR) operated in conventional mode. This fact is evidenced by the similar phosphorus removal efficiencies of the reactors. In addition, EDX analysis did not show any P adsorption on the structural matrix of the granules. This indicates that the values of phosphorus removal verified probably are due to biological activity and not to physical-chemical processes, such as precipitation.

3.4. Microbial community analysis

The metagenomic analysis found 26505 sequences in the seed sludge, 47276 in the control reactor (R1) and 74700 in the reactor supplemented with calcium (R2). The values of species richness and diversity indicators (Table 3) of R1 and R2 are significantly higher than those of the seed sludge, revealing that there was not a strong species selection by using simultaneous fill/draw mode SBRs.

He et al. (2016) operated a conventional SBR with anaerobic-oxic-anoxic (AOA) cycles in order to investigate the formation of denitrifying phosphorus-removing granules. They utilized a low ORL (0.3 kg $COD{\cdot}m^{-3}{\cdot}d^{-1}$), working with synthetic wastewater composed basically of acetate as the carbon source (150 mg L^{-1}), ammonia as the nitrogen source (15 mg L^{-1}), phosphorus (6 mg $TP{\cdot}L^{-1}$), magnesium (10 mg L^{-1}), and calcium (10 mg L^{-1}). The total cycle time was 8 h, and the aeration time (180-150 min) as well as the settling time (20-2min) were gradually reduced, while the anoxic phase (90–138 min) was extended, and the anaerobic phase was kept constant (180 min). Although the authors used an extremely low settling time, the richness and diversity of the mature granules were higher compared to the seed sludge.

On the other hand, Liu et al. (2017) investigated the addition of activated carbon, combined with the reduction of settling time, as a strategy to accelerate granulation in a conventional SBR (filling: 1 min; anaerobic stirring: 99 min; aeration: 150–175 min; settling: 30-5 min; decanting: 1 min). The authors worked with synthetic wastewater containing acetate as the carbon source (513 mg L^{-1}), ammonia and peptone as the nitrogen source (153 mg L^{-1}; 26 mg L^{-1}), phosphate (86.9 mg L^{-1}), magnesium (138 mg L^{-1}), and calcium (100 mg L^{-1}). A decrease in the species richness and diversity was observed.

These results seem to indicate that the microbial communities of AGS are very sensitive not only to the selection pressure imposed, but also to the type of SBR used, granulation strategies, duration of the experiment, aim of the research (simultaneous C, N and P, or not), type of substrate, and other operational conditions. Therefore, it is hard to predict such a behavior as it was observed in the present work.

Concerning the relative abundance of the microbial community at the level of phylum, Proteobacteria, Planctomycetes, Chloroflexi, Chlorobi, Bacteoidetes, and Acidobacterias were the dominant phyla in the seed sludge and the reactors (Fig. 4a). In fact, several studies have demonstrated that they are the most common phyla observed in AGS systems (Fan et al., 2018; Ou et al., 2018; Zhang et al., 2017).

Alphaproteobacteria and Deltaproteobacteria, which belong to the phylum Proteobacteria (Fig. 4b), account to a variety of families related to EPS production (Ramos et al., 2015). In R1, these groups accounted for abundances of 22% and 20% respectively, while in R2 the proportion was 52% and 2%. Although calcium addition to reactor R2 has favored Alphaproteobacteria compared to Deltaproteobacteria, the total abundance of the two groups together was equivalent in both reactors (R1: 42%, R2: 54%). This can explain the similar performances of the reactors in terms of EPS, since both microbial groups have comparable roles in the production of these polymers.

The taxonomic affiliation at the family level (Fig. 4c) was used to infer the functional groups related to the removal of C, N and P. The families were divided as AOB, DNB, GAOs, NOB, and PAOs (Fig. 5).

The abundance of AOB in the reactors was close to that observed for NOB (Fig. 5). This could suggest that ammonium and nitrite oxidations would have occurred at similar levels. However, by comparing Stages I and IV, a higher ammonium accumulation and a lower nitrite concentration in the effluent were found in Stage IV for both systems (Table 1). This can be explained by the fact that the conversion rate of ammonia to nitrite is generally slow, while nitrite is usually converted almost immediately to nitrate (Ekama and Wentzel, 2008). It is also important to notice that, with the shortage of dissolved oxygen caused by the biomass growth (see section 3.2), the ammonium oxidation would have been more affected, since this reaction is slower.

Hyphomonadaceae, Comamonadaceae, Dermabacteraceae, Planctomycetaceae, and Sinobacteraceae were the DNB families observed (Fig. 5). R1 and R2 showed a greater presence of DNB when compared to the seed sludge. The *Thauera* genus grew in abundance (seed sludge: 3%; R1: 15%; R2: 11%). This DNB genus is characterized for uptaking a wide range of organic substrates under aerobic conditions, which includes glucose, acetate, propionate, pyruvate, oleic acid, amino acid mixtures, and ethanol. Under denitrifying conditions, many substrates are consumed, with the exception of glucose and oleic acid (Thomsen et al., 2007).

The growth of DNB abundance in R1 and R2, in comparison with the seed sludge, seems to contradict the low denitrification levels observed

Table 3
Species richness and diversity indicators of microbial populations of AGS cultivated in the simultaneous fill/draw mode SBRs R1 (control) and R2 (supplemented with Ca^{2+}). Samples were collected on the 205th day of operation (Stage IV).

Sample	Good's Coverage (%)	Inverse Simpson	Shannon	Richness	Chao 1	ACE
Seed sludge	99.2	22.3	5.1	1731	1762	1838
R1	98.5	23.4	5.0	2736	3024	3275
R2	99.2	53.9	5.4	3401	3550	3792

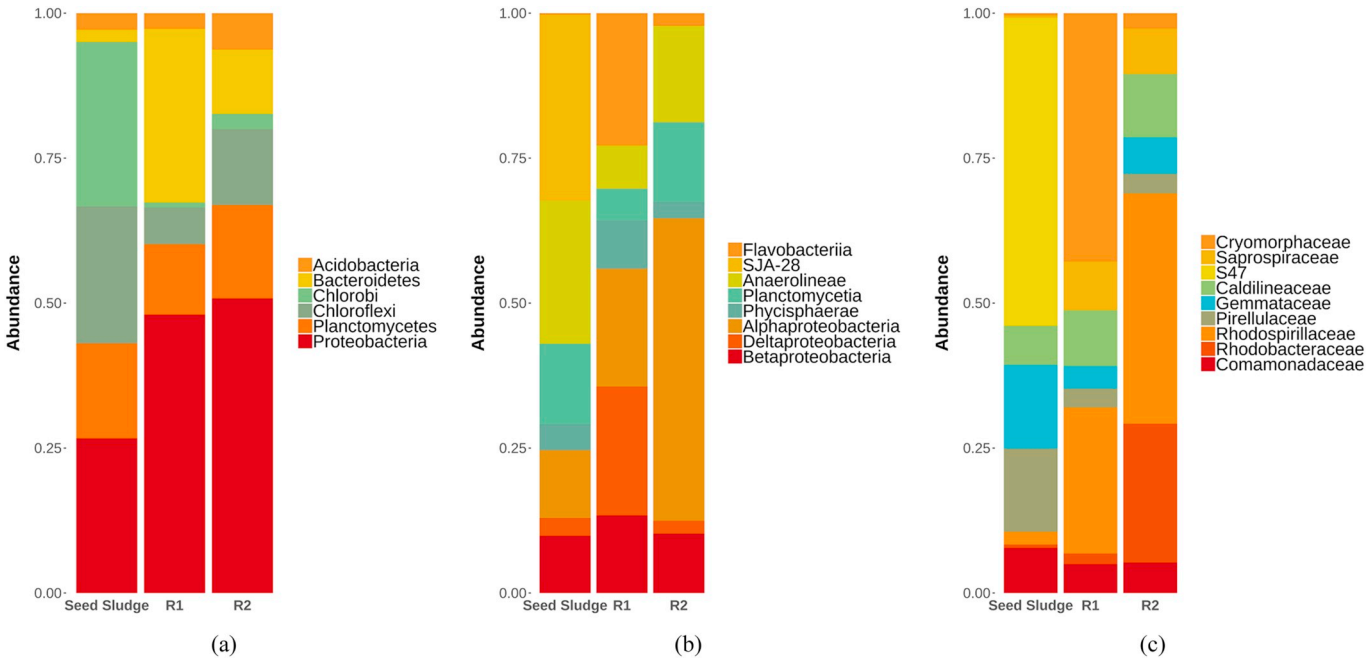

Fig. 4. Microbial community in the levels of phylum (a), class (b) and family (c) of the AGS cultivated in simultaneous fill/draw mode SBRs R1 (control) and R2 (supplemented with Ca^{2+}). Samples were collected on the 205th day of operation (Stage IV).

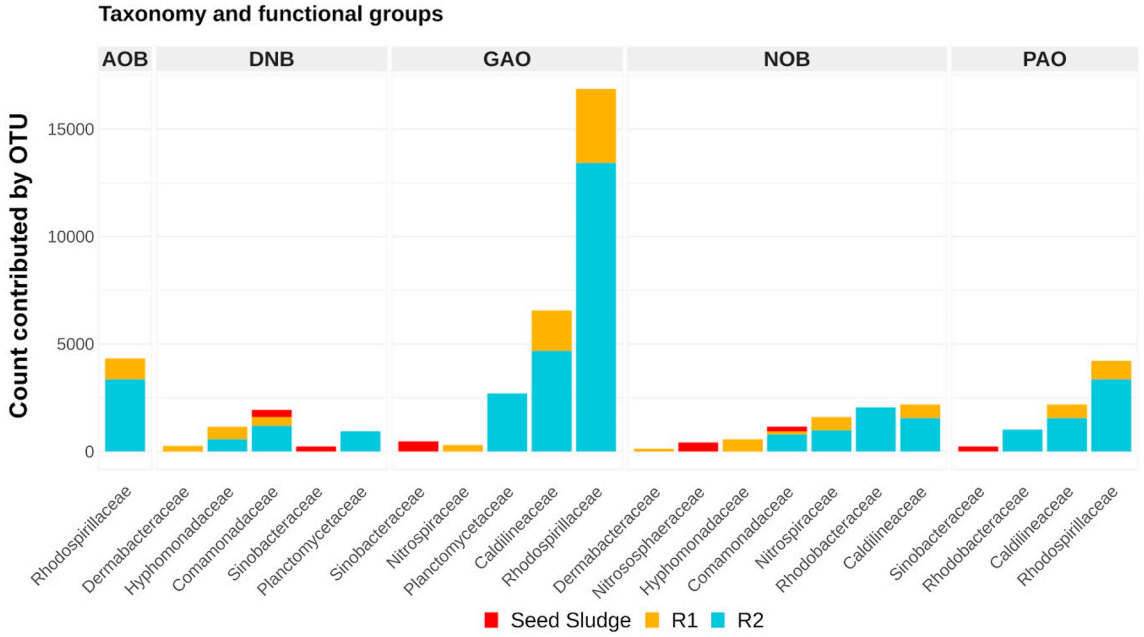

Fig. 5. Functional distribution of the taxonomical classification at family level of the AGS cultivated in simultaneous fill/draw mode SBRs R1 (control) and R2 (supplemented with Ca^{2+}). Samples were collected on the 205th day of operation (Stage IV).

(Table 1). A possible explanation is that, at the beginning of each cycle, there was plenty of substrate (ethanol), no oxygen and lots of NOx (due to accumulation from the previous cycle), resulting in a DNB growth. It is likely that DNB would consume most of the NOx available before the aerobic reaction step. When oxygen starts to be present again, the remaining substrate was consumed aerobically by ordinary heterotrophic bacteria, after which AOB and NOB could use the remaining oxygen for nitrification, increasing NOx concentration. However, denitrification could not take place due to the lack of substrate and the presence of oxygen. Therefore, NOx accumulates in the system, and the denitrification efficiency is low, even when DNB is abundant.

In relation to GAOs and PAOs, the abundance and diversity of the first microorganisms was considerably higher (Fig. 5), which corroborate the hypothesis that, in the anaerobic reaction step, the carbon source and the presence of NOx have favored DNB and GAOs over PAOs (see section 3.2). Additionally, since DNB and PAOs abundances are similar, it is possible that the competition between these organisms was less relevant compared to the competition between GAOs and PAOs.

Candidatus Alysiosphaera was also present in the AGS (R1: 0.63%; R2: 0.82%). They are responsible for degrading amino acids and several sugars, especially ethanol, being polyhydroxyalkanoates (PHA) consumers in anoxic environments (DPAOs) (Kragelund et al., 2006). Its

lower abundance indicates that DPAOs could not prevail over GAOs and DNB in the competition for substrate, which also contributed to the low efficiencies of denitrification and phosphorus removal found in both systems (Table 1).

4. Conclusions

In general, Ca^{2+} supplementation affected positively the sludge settleability, although a larger fraction of inert solids was found in the granules. The total EPS were the same for both reactors, and no remarkable differences were observed between their PS and PN contents.

Overall, Ca^{2+} addition in a simultaneous fill/draw mode SBR, operated with a low liquid upflow velocity ($0.92\ m\ h^{-1}$), neither accelerated the granule formation nor improved the operational performance. The microbial community structure, especially in terms of bioactivity, was not affected as well.

Therefore, the effect of divalent cations, such as Ca^{2+}, might be more pronounced in conventional SBRs, in which the selection pressure is higher.

Declaration of competing interest

None.

Acknowledgements

The authors would like to acknowledge the support obtained from the following Brazilian institutions: Conselho Nacional de Desenvolvimento Científico e Tecnológico – CNPq; Coordenação de Aperfeiçoamento de Pessoal de Nível Superior – CAPES; Fundação de Amparo à Pesquisa do Estado de Minas Gerais – FAPEMIG; Instituto Nacional de Ciência e Tecnologia em Estações Sustentáveis de Tratamento de Esgoto – INCT ETEs Sustentáveis (INCT Sustainable Sewage Treatment Plants); Central Analítica-UFC/CT-INFRA/MCTI-SISANO/Pró-Equipamentos CAPES; and Central de Genômica e Bioinformática (CeGenBio) do Núcleo de Pesquisa e Desenvolvimento de Medicamentos (NPDM).

Appendix A. Supplementary data

Supplementary data to this article can be found online at https://doi.org/10.1016/j.jenvman.2019.109850.

References

Adav, S.S., Lee, D.J., Show, K.Y., Tay, J.H., 2008. Aerobic granular sludge: recent advances. Biotechnol. Adv. 26, 411–423. https://doi.org/10.1016/j.biotechadv.2008.05.002.

APHA, 2012. Standard Methods for the Examination of Water and Wastewater, twenty-second ed. American Public Health Association, American Water Works Association, Water Environment Federation, Washington, DC.

Bassin, J.P., Kleerebezem, R., Dezotti, M., van Loosdrecht, M.C.M., 2012. Simultaneous nitrogen and phosphate removal in aerobic granular sludge reactors operated at different temperatures. Water Res. 46, 3805–3816. https://doi.org/10.1016/j.watres.2012.04.015.

Bengtsson, S., de Blois, M., Wilén, B.-M., Gustavsson, D., 2019. A comparison of aerobic granular sludge with conventional and compact biological treatment technologies. Environ. Technol. 40, 2769–2778.

Chuang, S.H., Ouyang, C.F., Wang, Y.B., 1996. Kinetic competition between phosphorus release and denitrification on sludge under anoxic condition. Water Res. 30, 2961–2968. https://doi.org/10.1016/S0043-1354(96)00201-1.

de Kreuk, M.K., 2006. Aerobic Granular Sludge: Scaling up a New Technology.

de Kreuk, M.K., Kishida, N., van Loosdrecht, M.C.M., 2007. Aerobic granular sludge - state of the art. Water Sci. Technol. 55, 75–81. https://doi.org/10.2166/wst.2007.244.

Derlon, N., Wagner, J., da Costa, R.H.R., Morgenroth, E., 2016. Formation of aerobic granules for the treatment of real and low-strength municipal wastewater using a sequencing batch reactor operated at constant volume. Water Res. 105, 341–350. https://doi.org/10.1016/j.watres.2016.09.007.

Ekama, G.A., Wentzel, M.C., 2008. Nitrogen removal. In: Henze, M., van Loosdrecht, M.C.M., Ekama, G.A., Brdjanovic, D. (Eds.), Biological Wastewater Treatment: Principles, Modelling and Design. IWA Publishing, p. 528.

Fan, X.Y., Gao, J.F., Pan, K.L., Li, D.C., Zhang, L.F., Wang, S.J., 2018. Shifts in bacterial community composition and abundance of nitrifiers during aerobic granulation in two nitrifying sequencing batch reactors. Bioresour. Technol. 251, 99–107. https://doi.org/10.1016/j.biortech.2017.12.038.

Girard, J.E., 2013. Principles of Environmental Chemistry, third ed. Jones & Bartlett Learning, Burlington.

He, Q., Zhou, J., Wang, H., Zhang, J., Wei, L., 2016. Microbial population dynamics during sludge granulation in an A/O/A sequencing batch reactor. Bioresour. Technol. 214, 1–8. https://doi.org/10.1016/j.biortech.2016.04.088.

Jiang, H.L., Tay, J.H., Liu, Y., Tay, S.T.L., 2003. Ca2+ augmentation for enhancement of aerobically grown microbial granules in sludge blanket reactors. Biotechnol. Lett. 25, 95–99. https://doi.org/10.1023/A:1021967914544.

Kończak, B., Karcz, J., Miksch, K., 2014. Influence of calcium, magnesium, and iron ions on aerobic granulation. Appl. Biochem. Biotechnol. 174, 2910–2918. https://doi.org/10.1007/s12010-014-1236-0.

Kragelund, C., Kong, Y., Waarde Der, J. van, Thelen, K., Eikelboom, D., Tandoi, V., Thomsen, T.R., Nielsen, P.H., 2006. Ecophysiology of different filamentous Alphaproteobacteria in industrial wastewater treatment plants. Microbiology 152, 3003–3012.

Li, X.-M., Liu, Q.-Q., Yang, Q., Guo, L., Zeng, G.-M., Hu, J.-M., Zheng, W., 2009. Enhanced aerobic sludge granulation in sequencing batch reactor by Mg^{2+} augmentation. Bioresour. Technol. 100, 64–67.

Liu, Y.Q., Moy, B., Kong, Y.H., Tay, J.H., 2010. Formation, physical characteristics and microbial community structure of aerobic granules in a pilot-scale sequencing batch reactor for real wastewater treatment. Enzym. Microb. Technol. 46, 520–525. https://doi.org/10.1016/j.enzmictec.2010.02.001.

Liu, X., Shen, Y., Qin, L., You, J., Chen, J., Chen, X., Tao, J., Li, B., 2017. Effect of granular activated carbon on the aerobic granulation of sludge and its mechanism. Bioresour. Technol. 236, 60–67. https://doi.org/10.1016/j.biortech.2017.03.106.

Liu, Y., Tay, J.H., 2002. The essential role of hydrodynamic shear force in the formation of biofilm and granular sludge. Water Res. 36, 1653–1665. https://doi.org/10.1016/S0043-1354(01)00379-7.

Liu, L., Gao, D.W., Zhang, M., Fu, Y., 2010. Comparison of Ca2+and Mg2+enhancing aerobic granulation in SBR. J. Hazard Mater. 181, 382–387. https://doi.org/10.1016/j.jhazmat.2010.05.021.

Lochmatter, S., Gonzalez-Gil, G., Holliger, C., 2013. Optimized aeration strategies for nitrogen and phosphorus removal with aerobic granular sludge. Water Res. 47, 6187–6197. https://doi.org/10.1016/j.watres.2013.07.030.

Long, B., Yang, C. zhu, Pu, W. hong, Yang, J. kuan, Jiang, G. sheng, Dan, J. feng, Li, C. yang, Liu, F. biao, 2014. Rapid cultivation of aerobic granular sludge in a pilot scale sequencing batch reactor. Bioresour. Technol. 166, 57–63. https://doi.org/10.1016/j.biortech.2014.05.039.

Mañas, A., Biscans, B., Spérandio, M., 2011. Biologically induced phosphorus precipitation in aerobic granular sludge process. Water Res. 45, 3776–3786. https://doi.org/10.1016/j.watres.2011.04.031.

Motteran, F., Pereira, E.L., Campos, C.M.M., 2013. The behaviour of an anaerobic baffled reACTOR (ABR) as the first stage in the biological treatment of hog farming effluents. Braz. J. Chem. Eng. 30, 299–310. https://doi.org/10.1590/S0104-66322013000200008.

Nereda, 2017. Aerobic Granular Sludge Demonstration. BACWA, Netherlands.

Nor-Anuar, A., Ujang, Z., Van Loosdrecht, M.C.M., De Kreuk, M.K., Olsson, G., 2012. Strength characteristics of aerobic granular sludge. Water Sci. Technol. 65, 309–316. https://doi.org/10.2166/wst.2012.837.

Ou, D., Li, H., Li, W., Wu, X., Wang, Y. qiao, Liu, Y. di, 2018. Salt-tolerance aerobic granular sludge: formation and microbial community characteristics. Bioresour. Technol. 249, 132–138. https://doi.org/10.1016/j.biortech.2017.07.154.

Pijuan, M., Werner, U., Yuan, Z., 2011. Reducing the startup time of aerobic granular sludge reactors through seeding floccular sludge with crushed aerobic granules. Water Res. 45, 5075–5083. https://doi.org/10.1016/j.watres.2011.07.009.

Pronk, M., de Kreuk, M.K., de Bruin, B., Kamminga, P., Kleerebezem, R., van Loosdrecht, M.C.M., 2015. Full scale performance of the aerobic granular sludge process for sewage treatment. Water Res. 84, 207–217. https://doi.org/10.1016/j.watres.2015.07.011.

Ramos, C., Suárez-Ojeda, M.E., Carrera, J., 2015. Long-term impact of salinity on the performance and microbial population of an aerobic granular reactor treating a high-strength aromatic wastewater. Bioresour. Technol. 198, 844–851. https://doi.org/10.1016/j.biortech.2015.09.084.

Ren, T.T., Liu, L., Sheng, G.P., Liu, X.W., Yu, H.Q., Zhang, M.C., Zhu, J.R., 2008. Calcium spatial distribution in aerobic granules and its effects on granule structure, strength and bioactivity. Water Res. 42, 3343–3352. https://doi.org/10.1016/j.watres.2008.04.015.

Rollemberg, S.L. de S., de Oliveira, L.Q., Barros, A.R.M., Melo, V.M.M., Firmino, P.I.M., dos Santos, A.B., 2019. Effects of carbon source on the formation, stability, bioactivity and biodiversity of the aerobic granule sludge. Bioresour. Technol. 278, 195–204. https://doi.org/10.1016/j.biortech.2019.01.071.

Schwarzenbeck, N., Borges, J.M., Wilderer, P.A., 2005. Treatment of dairy effluents in an aerobic granular sludge sequencing batch reactor. Appl. Microbiol. Biotechnol. 66, 711–718. https://doi.org/10.1007/s00253-004-1748-6.

Tay, J.H., Liu, Q.S., Liu, Y., 2001. The role of cellular polysaccharides in the formation and stability of aerobic granules. Lett. Appl. Microbiol. 33, 222–226. https://doi.org/10.1046/j.1472-765X.2001.00986.x.

Thomsen, T.R., Kong, Y., Nielsen, P.H., 2007. Ecophysiology of abundant denitrifying bacteria in activated sludge. FEMS Microbiol. Ecol. 60, 370–382. https://doi.org/10.1111/j.1574-6941.2007.00309.x.

Wan, J., Bessière, Y., Spérandio, M., 2009. Alternating anoxic feast/aerobic famine condition for improving granular sludge formation in sequencing batch airlift reactor

at reduced aeration rate. Water Res. 43, 5097–5108. https://doi.org/10.1016/j.watres.2009.08.045.

Wang, H., Song, Q., Wang, J., Zhang, H., He, Q., Zhang, W., Song, J., Zhou, J., Li, H., 2018. Simultaneous nitrification, denitrification and phosphorus removal in an aerobic granular sludge sequencing batch reactor with high dissolved oxygen: effects of carbon to nitrogen ratios. Sci. Total Environ. 642, 1145–1152. https://doi.org/10.1016/j.scitotenv.2018.06.081.

Wang, Q., Yao, R., Yuan, Q., Gong, H., Xu, H., Ali, N., Jin, Z., Zuo, J., Wang, K., 2018. Aerobic granules cultivated with simultaneous feeding/draw mode and low-strength wastewater: performance and bacterial community analysis. Bioresour. Technol. 261, 232–239. https://doi.org/10.1016/j.biortech.2018.04.002.

Zhang, D., Li, W., Hou, C., Shen, J., Jiang, X., Sun, X., Li, J., Han, W., Wang, L., Liu, X., 2017. Aerobic granulation accelerated by biochar for the treatment of refractory wastewater. Chem. Eng. J. 314, 88–97. https://doi.org/10.1016/j.cej.2016.12.128.